OncoTargets and Therapy

Dovepress
open access to scientific and medical research

Open Access Full Text Article

ORIGINAL RESEARCH

Clinical Significance And Integrative Analysis Of Kinesin Family Member 18B In Lung Adenocarcinoma

This article was published in the following Dove Press journal:
OncoTargets and Therapy

Yonglong Zhong[1,*]
Lingyu Jiang[2,*]
Xiaomao Long[1]
Yifan Zhou[1]
Shen Deng[1]
Hui Lin[1]
Xiangwei Li[1]

[1]Department of Thoracic Cardiovascular Surgery, The People's Hospital of Guangxi Zhuang Autonomous Region, Nanning, People's Republic of China; [2]Intensive Care Unit, The People's Hospital of Guangxi Zhuang Autonomous Region, Nanning, People's Republic of China

*These authors contributed equally to this work

Background: Kinesin family member 18B (KIF18B) is a member of the kinesin-8 superfamily, and functions as an oncogene in human cancers. However, its expression profile and role in lung adenocarcinoma (LUAD) remain unclear.

Materials and methods: We examined the expression profile of KIF18B using quantitative real-time reverse transcription polymerase chain reaction and immunohistochemistry in fresh clinical samples. Using data downloaded from the Cancer Genome Atlas database and Gene Expression Omnibus, we explored the clinical significance of KIF18B, potential mechanisms of its dysregulation and its underlying biological function in LUAD.

Results: KIF18B was significantly over-expressed in LUAD tissues relative to normal tissues. High KIF18B expression was associated with smoking history, positive nodal invasion, advanced clinical stage, death status and poorer prognosis. Cox regression analyses revealed that KIF18B overexpression was an independent prognostic biomarker for poor overall survival (OS) and recurrence-free survival in LUAD. In addition, KIF18B mutation was observed in 2.2% of LUAD cases. DNA copy number variation was correlated with upregulated expression of KIF18B in LUAD tissues and cell lines. The methylation level of some KIF18B DNA CpG sites was negatively associated with its mRNA expression. KIF18B was predictively targeted by miR-125a-5p, which was downregulated in LUAD tissues, inversely correlated with KIF18B mRNA expression and significantly associated with poor OS. Furthermore, gene set enrichment analysis revealed that genes positively co-expressed with KIF18B were mainly enriched in cell cycle signaling pathways.

Conclusion: Our results indicate that KIF18B is a promising prognostic biomarker for LUAD. DNA amplification, hypomethylation as well as miR-125a-5p downregulation may be involved in the mechanism of KIF18B dysregulation in LUAD. KIF18B might function as a novel oncogene through cell cycle regulation pathways in LUAD.

Keywords: lung adenocarcinoma, kinesin, prognosis, miR-125a-5p, bioinformatic analysis

Introduction

Lung cancer is one of the most prevalent malignancies and is a major leading cause of cancer-related death worldwide.[1] As the main pathological subtype of lung cancer, lung adenocarcinoma (LUAD) has high morbidity and poor outcomes. Great improvements have been made in LUAD diagnosis and treatment over the past decade, but the long-term survival rate of patients with LUAD is still low.[2] Although high-throughput sequencing analysis has facilitated genetic and epigenetic research in lung cancer, the molecular mechanisms involved are not yet fully elucidated.

Correspondence: Hui Lin; Xiangwei Li
Department of Thoracic Cardiovascular Surgery, The People's Hospital of Guangxi Zhuang Autonomous Region, No. 6 Taoyuan Road, Nanning 530021, People's Republic of China
Tel/fax +867712186524
Email linhui33622@126.com; 18277156688@139.com

submit your manuscript | www.dovepress.com
DovePress
http://doi.org/10.2147/OTT.S227438

Kinesin superfamily proteins (KIFs) are a class of microtubule-dependent molecular motor proteins.[3] They share a conserved motor domain and participate in some intracellular and extracellular functions, such as mitosis, cell proliferation, apoptosis, motility and substance transportation. So far, more than 14 subfamilies including more than 30 KIFs have been reported. Increasing evidence has shown that various KIFs are over-expressed in multiple malignancies and they are involved in tumor growth and development.[4] In our previous study, we firstly found that KIF18A, a member of the kinesin-8 proteins, confers a malignant phenotype in LUAD and predicts an unfavorable outcome in LUAD patients.[5] The KIF18B gene, a homolog of the KIF18A gene, is located on chromosome 17q21.31 and consists of 17 exons. Its encoded protein also belongs to the kinesin-8 subfamily and is a novel dynamics regulatory protein that interacts with EB1 to regulate astral microtubule length during mitosis.[6] Recent reports have revealed that KIF18B is over-expressed in several tumors, such as cervical cancer[7] and hepatocellular carcinoma,[8] and it acts as a cancer-related driver gene. However, the expression profiles and role of KIF18B in lung cancer remain unclear.

In the current study, we explored the expression profiles of KIF18B in clinical samples as well as the Cancer Genome Atlas (TCGA) database and the Gene Expression Omnibus (GEO) database to evaluate its clinical significance in LUAD. In addition, we investigated the possible molecular mechanism of KIF18B dysregulation and its underlying biological function in LUAD by performing a bioinformatics analysis.

Materials And Methods

Tissue Sample Collection

From December 2017 to March 2018, 22 pairs of LUAD and normal lung tissue (>5 cm away from tumors) specimens were obtained from 22 patients who underwent surgical resection. For reverse transcription and quantitative polymerase chain reaction (qPCR), the fresh tissue samples were snap frozen using liquid nitrogen and stored at −80°C. All cancer specimens were histologically classified as LUADs. The current study was approved by the Ethics Committees/Institutional Review Boards of the People's Hospital of Guangxi Zhuang Autonomous Region, and all participants provided written informed consent in accordance with the Declaration of Helsinki.

Real-Time Quantitative Polymerase Chain Reaction

Total RNA was isolated from frozen tissue specimens using Trizol reagent (Invitrogen, Carlsbad, CA, USA) and reverse-transcribed using the Fast Quant RT Kit (with gDNase) (Tiangen Biotech, Beijing, China) in accordance with the manufacturer's instructions. Quantitative polymerase chain reaction (qPCR) was performed using SuperReal PreMix Plus (SYBR Green) (Tiangen Biotech, Beijing, China) and an ABI 7500 Real-Time PCR System (Applied BioSystems, Foster City, USA). The qPCR cycling conditions included an initial denaturation step at 95°C for 15 min, followed by 40 cycles of denaturation at 95°C for 10 s, and a primer annealing/extension at 56°C for 32 s. KIF18B mRNA expression levels were normalized to those of GAPDH and analyzed using the $2^{-\triangle\triangle}$ method. The primers sequences were as follows:

KIF18B, sense primer 5′-GCTGCAAGTAGTGGTAC GGG-3′ and anti-sense primer 5′-CCTCAGGGTTAAAC ACCAGCA-3′;

GAPDH, sense primer 5′-CATGAGAAGTATGACAA CAGCCT-3′ and anti-sense primer 5′-AGTCCTTCCACG ATACCAAAG-3′.

Immunohistochemistry Assay

An immunohistochemistry (IHC) assay was performed to detect KIF18B protein expression in the tissue samples. After excision, the surgical specimens were immediately immersed in 10% formalin for fixation, followed by dehydration, paraffin embedding and sectioning. After dewaxing, rehydration, antigen retrieval and blocking of endogenous peroxidase activity, the slides were incubated with an anti-KIF18B antibody (1:100, Abcam, Cambridge, UK) at 4°C overnight. For negative controls, the primary antibody was replaced with PBS. After washing with PBS, the slides were incubated with a biotinylated goat anti-rabbit secondary antibody (Maixin Biotech, Fuzhou, China) for 15 min at room temperature, and then stained with diaminobenzidine tetrahydrochloride. Image pro plus 6.0 software (Media Cybernetics, Inc., Silver Spring, MD, USA) was used to quantitatively analyze the degree and proportion of KIF18A staining. The integrated optical density (IOD) and area of interest (AOI) were measured and the mean density (IOD/AOI) was calculated to evaluate specific protein expression. The results were re-checked by two independent pathologists from the

Department of Pathology of the People's Hospital of Guangxi Zhuang Autonomous Region.

Data Mining In LUAD Tissues And Cells

Pan-cancer KIF18B expression was analyzed using UALCAN (http://ualcan.path.uab.edu/),[9] which is a comprehensive and interactive web resource for analyzing cancer OMICS data. Level 3 data for patients with primary LUAD were obtained from TCGA (https://cancergenome.nih.gov/). KIF18B expression profiles were collected for 514 primary LUAD samples and 59 normal controls. Among the 514 patients, there was complete clinical and follow-up information for 502 cases. Data including age, gender, smoking history, tumor size, nodal invasion status, TNM stage, residual tumors, recurrence status, recurrence-free survival (RFS) in days, living status and overall survival (OS) in days, were extracted. A total of three lung cancer gene microarray datasets (GSE31210, GSE50081 and GSE30219) downloaded from the GEO (https://www.ncbi.nlm.nih.gov/geo/)[10] were used for validation.

To explore the mechanism of KIF18B dysregulation in LUAD, its gene-level thresholded gistic2-processed copy number variation (CNV) (n=511) and DNA methylation status (methylation 450 k) (n=453) were collected from TCGA simultaneously.

KIF18B mRNA expression, copy number and DNA methylation in LUAD cell lines were obtained from the cancer cell line encyclopedia (CCLE) (https://portals.broadinstitute.org/ccle),[11,12] which is an online database that provides public access to genomic data (including gene expression, gene methylation, mutation data), analysis and visualization for over 1100 cell lines.

Predicting The Regulatory miRNAs Of KIF18B

The predicted and validated regulatory miRNAs of the KIF18B gene were obtained from six databases: miRwalk (http://129.206.7.150),[13] miRDB (http://www.mirdb.org),[14] Tarbase (http://carolina.imis.athena-innovation.gr),[15] DIANA-microT (http://diana.imis.athena-innovation.gr),[16] TargetScan (http://www.targetscan.org/vert_72/),[17] and starBase (http://starbase.sysu.edu.cn).[18] The miRNA-seq data for LUAD tissues and normal lung tissues were collected from TCGA. Differentially expressed miRNAs between primary tumors and normal controls were identified using the edgeR package with a cut-off of $|\log^2$ (fold change) $|>1$ and P-value <0.05. All the downregulated miRNAs in the TCGA-LUAD samples were used as a subset. The overlapping miRNAs among the six databases and the TCGA subset were defined as potential regulatory miRNAs of the KIF18B gene in LUAD.

Identification Of Genes Differentially Expressed In Correlation With KIF18B In LUAD

LinkedOmics (http://www.linkedomics.org),[19] a new publicly available portal for multi-omics data from all 32 TCGA cancer types, was used to identify genes differentially expressed in correlation with KIF18B in TCGA-LUAD. A Benjamini and Hochberg false discovery rate (FDR) <0.01 and a P-value <0.05 were set as the cut-off criteria. The top three genes positively correlated with KIF18B were selected for further analysis. GEPIA2 (http://gepia2.cancer-pku.cn),[20] an online interactive web server for analyzing the RNA sequencing data of tumors and normal samples from the TCGA and GTEx projects, was used to analyze the expression profiles and prognostic value of selected genes. Patients with LUAD were grouped by the median values of mRNA expression. $P<0.05$ was considered statistically significant.

Functional And Pathway Enrichment Analysis

Gene set enrichment analysis (GSEA) was performed using the LinkInterpreter module of LinkedOmics to explore gene ontology (GO) (including cellular components, molecular function and biological processes) and signaling pathway enrichment analyses of genes co-expressed with KIF18B. FDR < 0.05 and a P-value <0.05 were considered statistically significant.

Statistical Analysis

Statistical analysis was performed using the SPSS 20.0 software package (SPSS Inc., Chicago, IL, USA). The association between KIF18B mRNA expression and clinicopathological features was evaluated using Welch's t-tests. The diagnostic and prognostic value of KIF18B expression in LUAD was judged using receiver operating characteristic (ROC) curves. Kaplan–Meier curves of OS and RFS were generated using GraphPad Prism (GraphPad Software, CA, USA). Log rank tests and Cox regression analysis were performed in different data cohorts individually. $P<0.05$ was considered statistically significant.

Results

KIF18B Was Significantly Upregulated In LUAD

We performed a qPCR assay to detect KIF18B mRNA expression in 22 paired fresh LUAD tissue samples and non-cancer tissue samples. The results showed that KIF18B mRNA expression in LUAD tissues was higher than that in corresponding normal lung tissues (Figure 1A). Moreover, we performed an IHC assay with these samples to examine the expression of KIF18B protein. Very weak KIF18B staining was observed in normal lung epithelia (Figure 1B, upper), whereas moderate and strong KIF18B staining was detected in most malignant cells (Figure 1B, lower). Compared with normal tissues, KIF18B expression

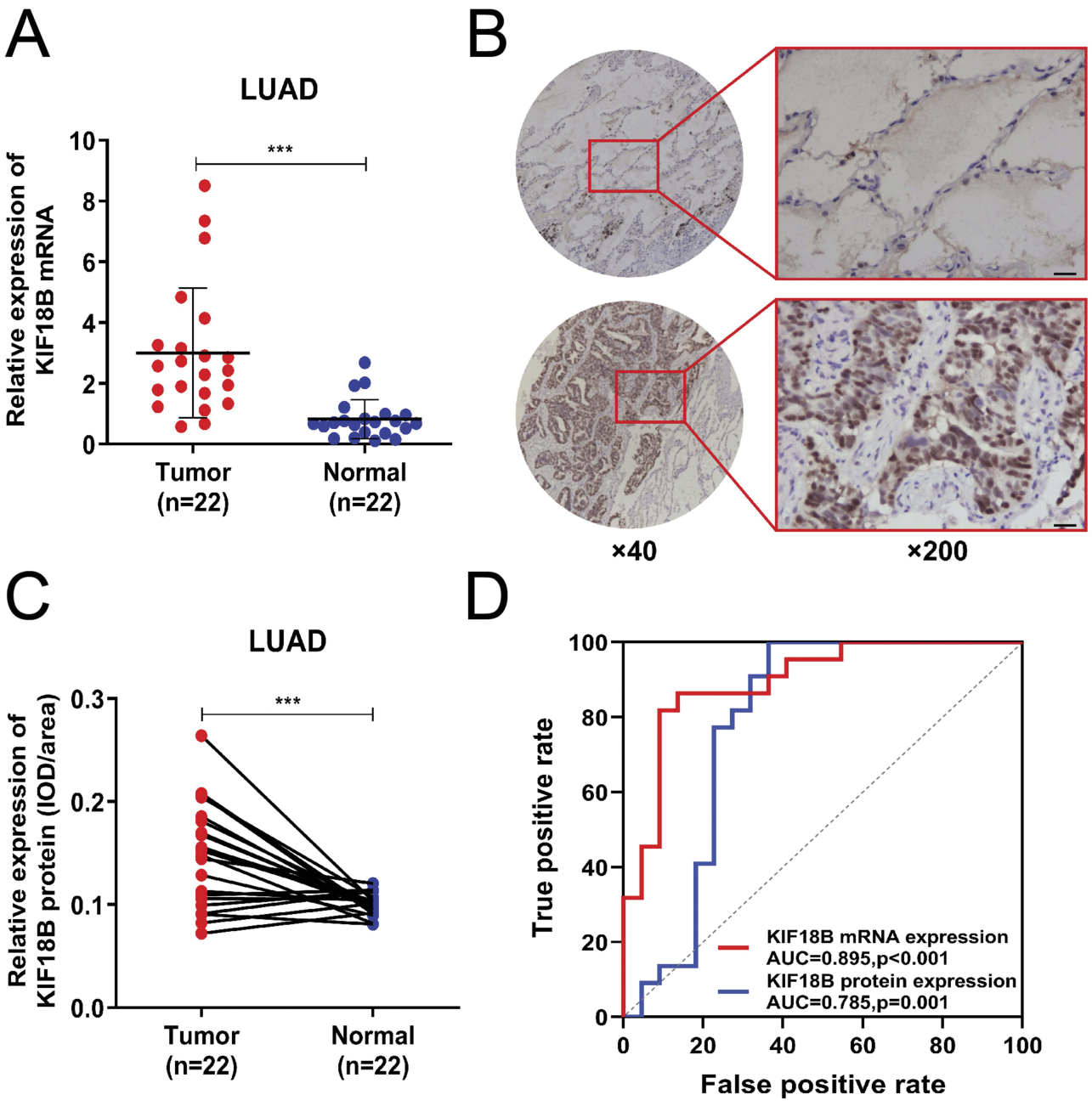

Figure 1 Expression of KIF18B mRNA and protein in fresh LUAD. (**A**) KIF18B mRNA expression was examined using qPCR in tumor tissues and paired normal lung tissues. GAPDH expression served as an internal control. (**B**) KIF18B protein expression was detected through IHC (upper panel, normal lung tissue; lower panel, tumor tissue). (**C**) Comparison of KIF18B expression between tumor tissue and paired normal lung tissue was performed through a semi-quantitative analysis. (**D**) The diagnostic value of KIF18B expression in LUAD was evaluated using ROC curves (red curve, mRNA expression of KIF18B; blue curve, protein expression of KIF18B). ***P<0.001.
Abbreviations: KIF18B, Kinesin family member 18B; LUAD, lung adenocarcinoma; IHC, immunohistochemistry; ROC, receiver operating characteristic.

was significantly increased in tumor tissues (Figure 1C). The qPCR and IHC results were used to evaluate the diagnostic value of KIF18B in LUAD using ROC curves. The area under curve (AUC) value of KIF18B overexpression at the mRNA and protein level for LUAD diagnosis was 0.895 and 0.785, respectively (Figure 1D).

By data mining using UALCAN, we characterized KIF18B mRNA expression in 24 tumor types compared with corresponding normal controls. As shown in Figure 2A, KIF18B mRNA expression was markedly elevated in most of the human solid tumors including LUAD (dotted box). We also extracted RNA-seq data from TCGA-LUAD for further analysis. The GSE31210 and GSE30219 array sets were used for verification. The results showed that KIF18B mRNA expression was significantly higher in tumor tissues (n=514) compared with normal lung tissues (n=59) (Figure 2B). The above results were also validated in the samples from the GSE31210 and GSE30219 array sets (Figure 2C and D). Moreover, the AUC value of KIF18B expression for LUAD diagnosis was 0.976 in the TCGA cohort (Figure 2E). The diagnostic value of KIF18B in LUAD was also confirmed in the GSE31210 and GSE30219 array sets (Figure 2E).

High KIF18B Expression Was Associated With Unfavorable Outcomes In LUAD Patients

To explore the expression distribution of KIF18B, we examined the expression pattern of KIF18B in different clinicopathological parameter subgroups, as defined using TCGA. The results showed that KIF18B was significantly upregulated in cases younger than or equal to 65 years old (P=0.001), males (P=0.030), smokers (P=0.008), positive nodal invasion cases (P=0.005), advanced clinical stage

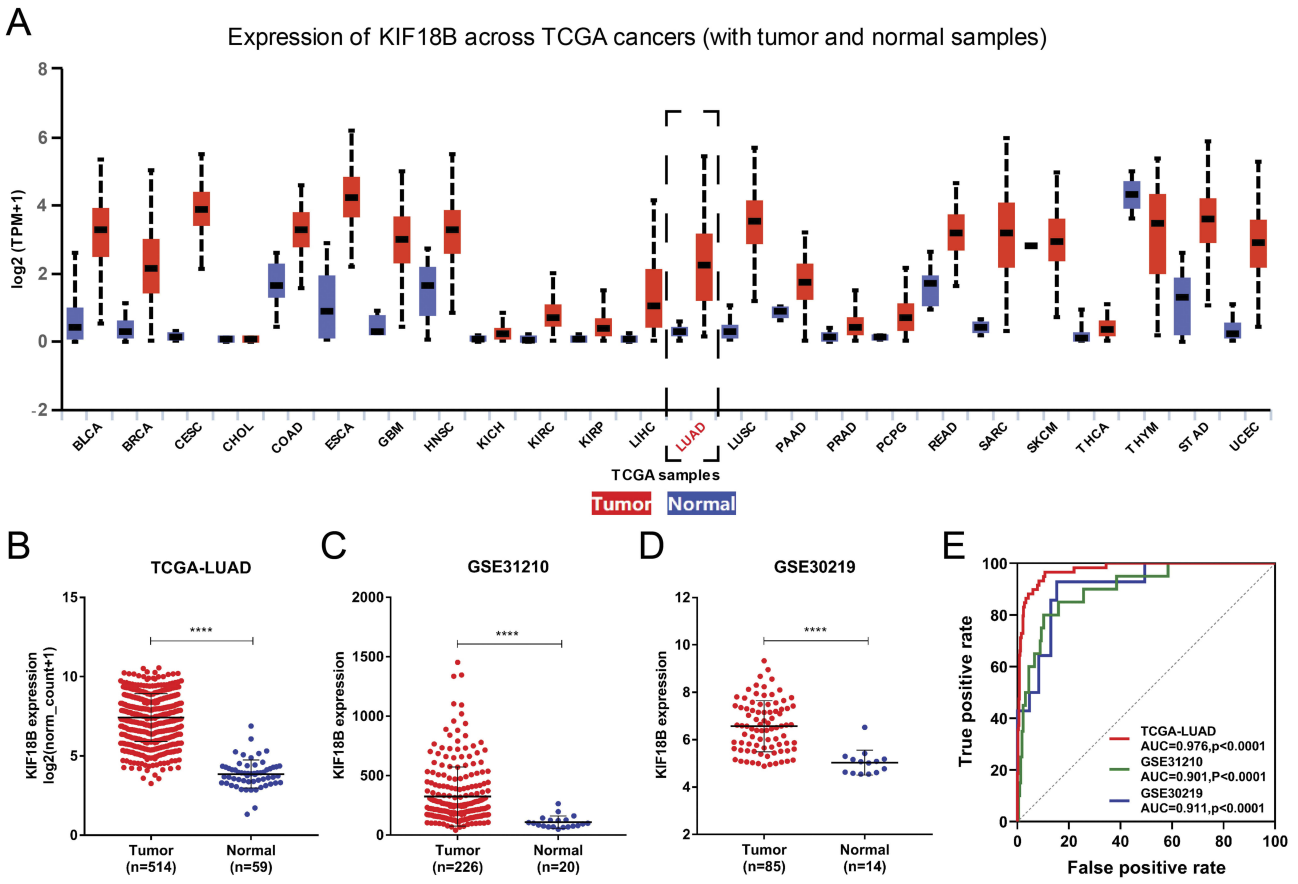

Figure 2 KIF18B mRNA expression profiles in patients with LUAD both in TCGA and GEO dataset cohorts. (**A**) Expression of KIF18B across TCGA tumors compared with normal tissue samples. (**B**–**D**) KIF18B mRNA expression in LUAD tissues and normal controls from a TCGA cohort (**B**), GSE31210 cohort (**C**) and GSE30219 cohort (**D**). (**E**) ROC curves showing the diagnostic value of KIF18B in LUAD (red curve, data from TCGA cohort; green curve, data from GSE31210 cohort; blue curve, data from GSE30219 cohort). ****P<0.0001.

Abbreviations: KIF18B, Kinesin family member 18B; LUAD, lung adenocarcinoma; TCGA, the Cancer Genome Atlas; GEO, Gene Expression Omnibus; ROC, receiver operating characteristic.

(P=0.021) and deceased cases (P=0.006) compared with their respective counterparts (Table 1). Otherwise, we found that tumor size, residual tumor status and recurrence status were not associated with high KIF18B expression.

To examine the correlation between KIF18B expression and survival outcomes in patients with LUAD, we analyzed clinical survival data from TCGA. Patients with primary LUAD were divided into high and low KIF18B expression groups using median values of KIF18B mRNA expression. Firstly, using OS as an outcome indicator, the results showed that high KIF18B expression was significantly associated with shorter OS in primary LUAD patients (P=0.0023; Figure 2A). Interestingly, when using GEO database data for validation, we also found that the high KIF18B expression group had significantly poorer OS compared with the low KIF18B expression group in the GSE31210, GSE50081 and GSE30219 array sets (P=0.0004, P=0.0003 and P=0.0071, respectively; Figure 3B–D). Kaplan–Meier curves of RFS using TCGA-LUAD cohorts showed that there was no significant association between KIF18B expression and RFS in LUAD patients (P=0.4030; Figure 3E). However, we found that in the GSE31210 (P<0.0001), GSE50081 (P=0.0340) and GSE30219 (P=0.0005) datasets, LUAD patients with higher KIF18B expression had remarkably shorter RFS compared with patients with low KIF18B expression (Figure 3F–H).

Table 1 Correlation Between The Clinicopathological Parameters And KIF18B Expression In Lung Adenocarcinoma

Parameters	Variables	KIF18B mRNA Expression	t	*P*-value
Age (years)	> 65 ≤ 65	7.2027±1.4277 7.6653±1.5511	−3.445	0.001
Gender	Male Female	7.5824±1.5419 7.2877±1.4763	2.176	0.030
Smoking history	Non-smoker Smoker	6.9982±1.5697 7.5128±1.4990	0.709	0.008
T classification	T1–2 T3–4	7.4558±1.5289 7.4242±1.4153	−0.007	0.994
Nodal invasion	No Yes	7.3107±1.5651 7.6981±1.3570	−2.841	0.005
Clinical stage	I/II III/IV	7.3592±1.5460 7.3592±1.5460	−2.328	0.021
Residual tumors	R0 R1/R2	7.4465±1.5009 7.4465±1.5009	−0.936	0.361
Recurrence status	No Yes	7.4458±1.4208 7.4458±1.4208	0.184	0.854
Living status	Living Dead	7.2870±1.5669 7.2870±1.5669	2.774	0.006

Notes: R0: no residual tumor; R1: microscopic residual tumor; R2: macroscopic residual tumor.

Moreover, to further investigate the independent prognostic value of KIF18B in terms of OS, univariate and multivariate analyses based on the Cox regression model were conducted (Figure 4A). The results from the TCGA-LUAD dataset showed that advanced clinical stage, the presence of residual tumors and increased KIF18B expression were associated with unfavorable OS. Multivariate analysis confirmed that KIF18B expression was an independent prognostic factor for predicting unfavorable OS in LUAD, after adjustment of clinical stage, nodal status and residual tumors. Subsequently, we performed the same analysis using the genomic data from the GEO database for validation. The results also confirmed that increased KIF18B expression was linked to poorer OS and was an independent prognostic indicator.

Similarly, we performed Cox regression analyses on the above cohorts in terms of RFS. The following multivariate analysis also confirmed that in the three independent GEO database cohorts, but not the TCGA cohort, increased KIF18B expression was an independent prognostic biomarker for poor RFS in patients with LUAD (Figure 4B).

Finally, given that KIF18B expression was linked to patient survival outcomes, a ROC curve analysis was performed to explore the prognostic value of KIF18B mRNA expression. As shown in Figure 5, the AUC of KIF18B expression in TCGA-LUAD for predicting OS and RFS was 0.561 and 0.591, respectively. For validation, the AUC of KIF18B expression in predicting OS was 0.842, 0.772 and 0.743 in datasets from the GSE31210, GSE50081 and GSE30219 array sets, respectively (Figure 5A). In term of predicting RFS, the AUC of KIF18B expression in datasets from the GSE31210, GSE50081 and GSE30219 array sets was 0.918, 0.764 and 0.787, respectively (Figure 5B).

KIF18B Expression Was Modulated By DNA Amplification And DNA Hypomethylation

We attempted to explore the underlying mechanism of KIF18B gene dysregulation in LUAD using deep sequencing data from TCGA-LUAD. Firstly, we examined copy number alterations in TCGA-LUAD using

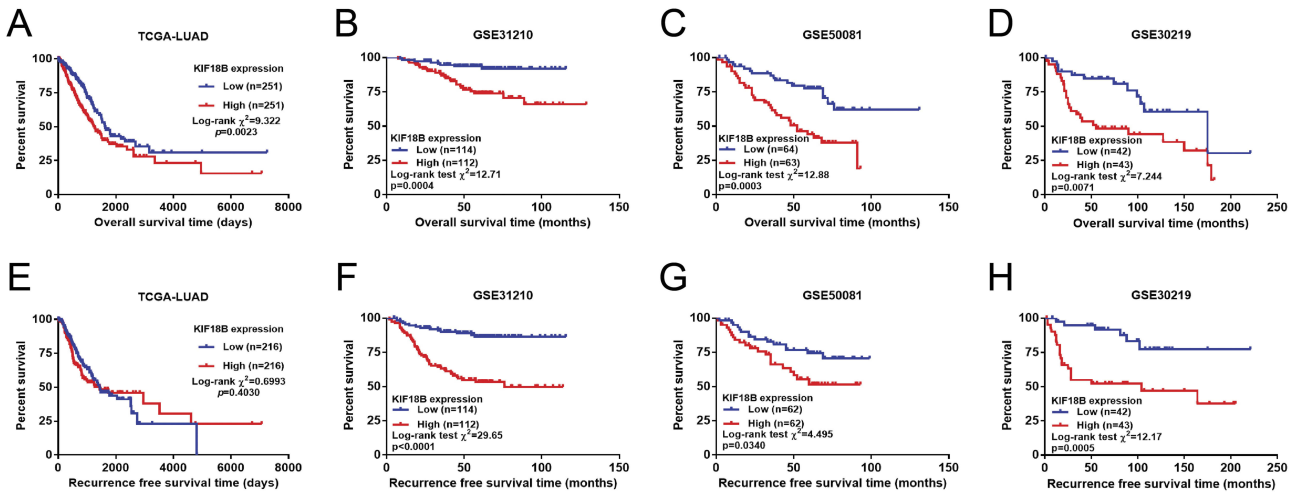

Figure 3 Kaplan–Meier curves of OS and RFS in LUAD based on the mRNA expression of KIF18B. (**A**–**D**) Kaplan–Meier curves of OS in all patients with primary LUAD, using data from TCGA-LUAD (**A**), GSE31210 (**B**), GSE50081 (**C**), and GSE30219 (**D**). (**E**–**H**) Kaplan–Meier curves of RFS in all patients with primary LUAD, using data from TCGA-LUAD (**E**), GSE31210 (**F**), GSE50081 (**G**), and GSE30219 (**H**). Patients in individual cohorts were grouped using median KIF18B mRNA expression.
Abbreviations: OS, overall survival; RFS, recurrence-free survival; LUAD, lung adenocarcinoma; KIF18B, Kinesin family member 18B; TCGA, the Cancer Genome Atlas.

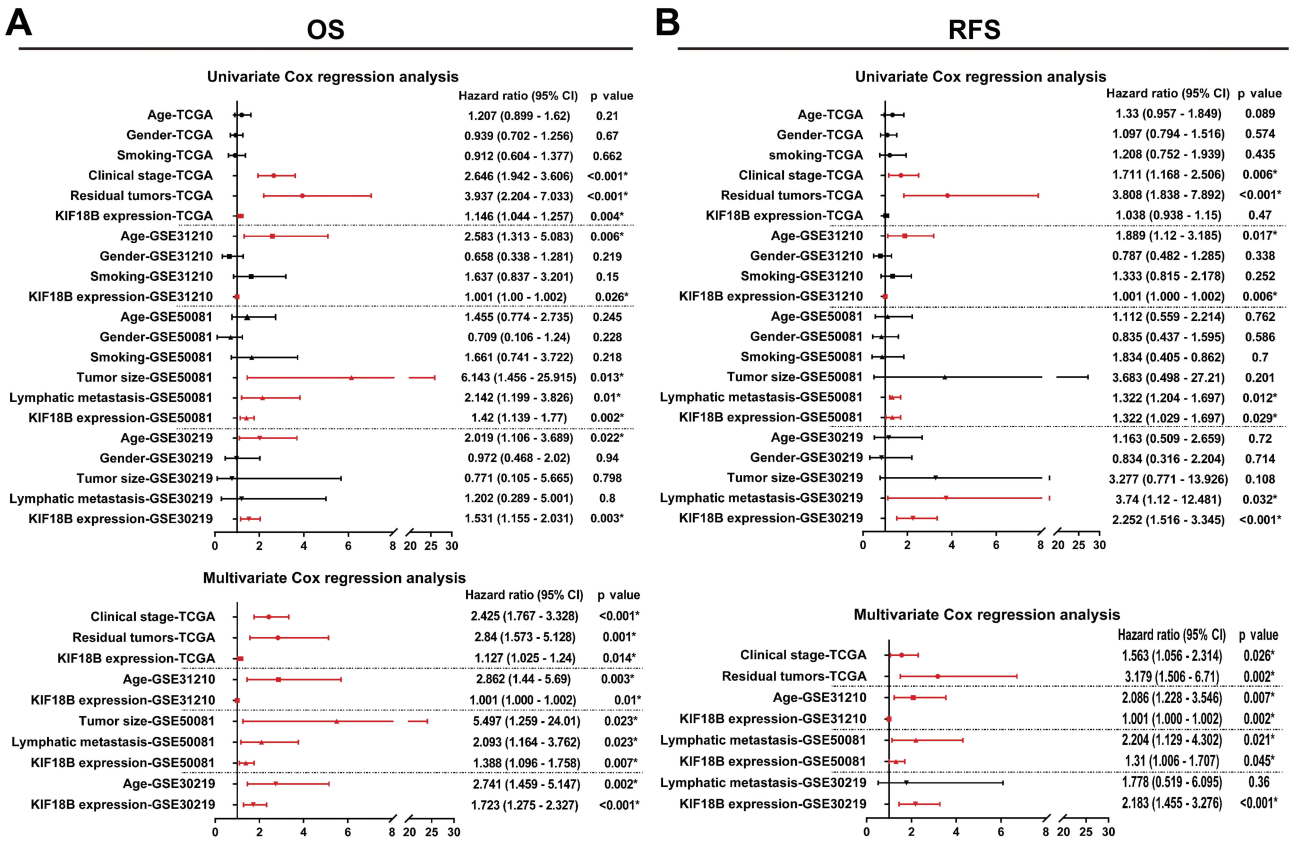

Figure 4 Forest maps of Cox regression analysis. (**A**) Forest maps showing univariate and multivariate analysis of OS in patients with LUAD. (**B**) Forest maps showing univariate and multivariate analysis of RFS in patients with LUAD. *P<0.05.
Abbreviations: OS, overall survival; RFS, recurrence-free survival; LUAD, lung adenocarcinoma.

cBioPortal (https://www.cbioportal.org) for Cancer Genomics. KIF18B gene alteration was observed in 2.2% of LUAD cases (n=5) with sequencing and DNA copy number alteration data (n=230) (Figure 6A). Missense mutations, truncating mutations as well as gene amplification were the main types of KIF18B

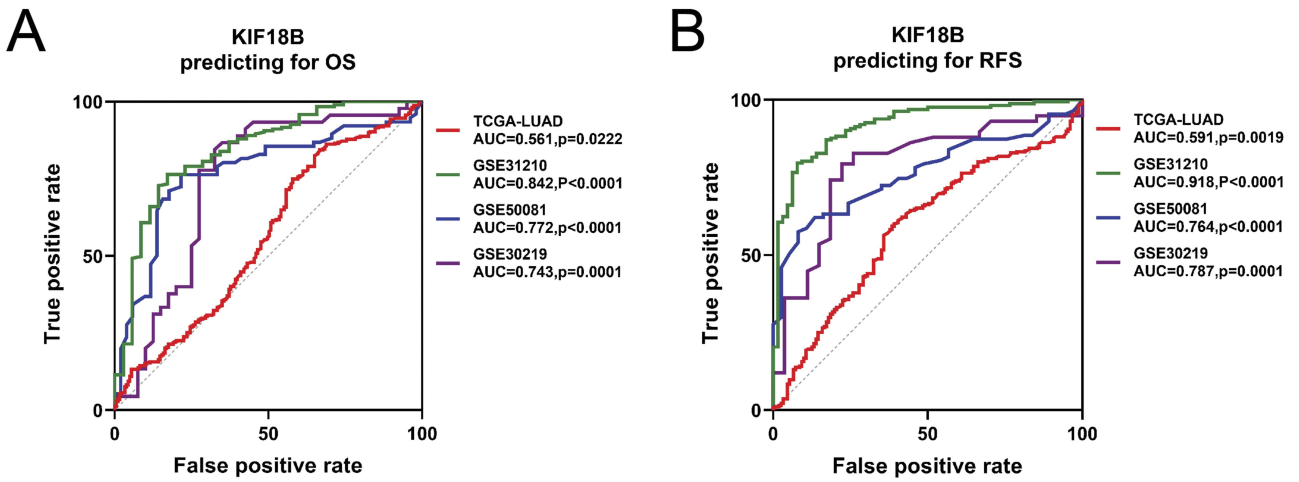

Figure 5 ROC curves of KIF18B expression to predict OS and RFS in LUAD. (**A**) ROC curves of KIF18B mRNA expression to predict OS in LUAD. (**B**) ROC curves of KIF18B mRNA expression to predict RFS in LUAD. Red curves, TCGA-LUAD cohort; green curves, GSE31210 datasets; blue curves, GSE50081 datasets; purple curves, GSE30219 datasets.

Abbreviations: ROC, receiver operating characteristic; KIF18B, Kinesin family member 18B; OS, overall survival; RFS, recurrence-free survival; LUAD, lung adenocarcinoma; TCGA, the Cancer Genome Atlas.

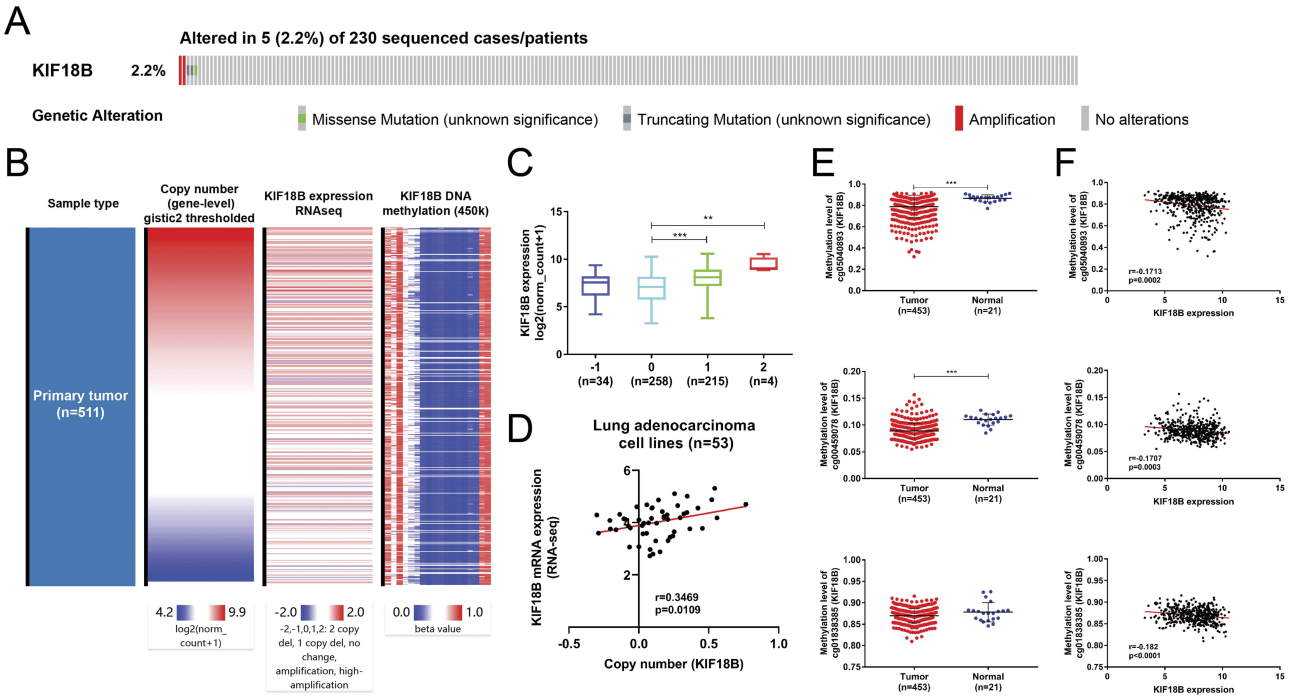

Figure 6 KIF18B gene alterations and DNA methylation in LUAD. (**A**) Genetic alteration of KIF18B in 230 cases of LUAD. (**B**) Heatmap of KIF18B mRNA expression (RNA-seq), CNV (gistic2 thresholded) and DNA methylation (450 k) in patients with primary LUAD; −2: homozygous deletion; −1: heterozygous loss, 0: copy neutral; +1: low-level copy gain; +2: high-level amplification. (**C**) KIF18B CNVs and mRNA expression in LUAD tumor tissues. (**D**) KIF18B copy number and mRNA expression in LUAD cell lines (n = 53). (**E**) Scatter plots showing the KIF18B DNA methylation levels of three CpG positions in LUAD tumor tissues and normal lung tissues. (**F**) Regression analysis of KIF18B mRNA expression and DNA methylation levels of three CpG positions. ***P*<0.01, ****P*<0.001.

Abbreviations: KIF18B, Kinesin family member 18B; LUAD, lung adenocarcinoma; CNV, copy number variation.

gene alteration. Then, we evaluated KIF18B mRNA expression, DNA CNVs and methylation in a total of 511 LUAD patients simultaneously. The heatmap of KIF18B mRNA expression, CNVs and DNA methylation is shown in Figure 6B. Among the cohort with measured CNVs, 219 cases (42.86%) had DNA amplification (+1: low-level amplification, n=215; +2: high-level amplification, n=4), while 34 cases (6.35%) had DNA deletion; DNA amplification was significantly associated with upregulated KIF18B mRNA expression

(Figure 6C). We also examined KIF18B expression and copy number data in 53 LUAD cell lines from the CCLE. Regression analysis indicated a significant positive correlation between KIF18B mRNA expression and copy number (Figure 6D). Finally, KIF18B mRNA expression and DNA methylation were measured at the same time in a total of 453 primary LUAD cases and 21 normal controls. The results showed that with the exception of cg01838385, two CpG sites (cg05040893, cg00459078) in the KIF18B gene were generally hypomethylated in tumor tissues, but not in normal lung tissues (Figure 6E). Regression analyses were performed to evaluate the relationship between KIF18B mRNA expression and the methylation of three CpG sites. As shown in Figure 6F, KIF18B expression was negatively associated with DNA methylation in the selected CpG sites (all $P<0.05$).

KIF18B Was Predictively Targeted By Mir-125a-5p In LUAD

To explore the potential regulatory miRNAs of KIF18B in LUAD, we examined the miRNA-seq data of primary LUAD tissues and normal lung tissues extracted from the TCGA-LUAD dataset. Differentially expressed miRNAs are shown in Figure 7A, and a total of 70 downregulated miRNAs as well as 116 upregulated miRNAs were identified. The potential regulatory miRNAs of KIF18B were obtained from public databases including miRwalk, miRDB, Tarbase, DIANA-microT, TargetScan, and starBase. Among these six datasets and the TCGA cohort

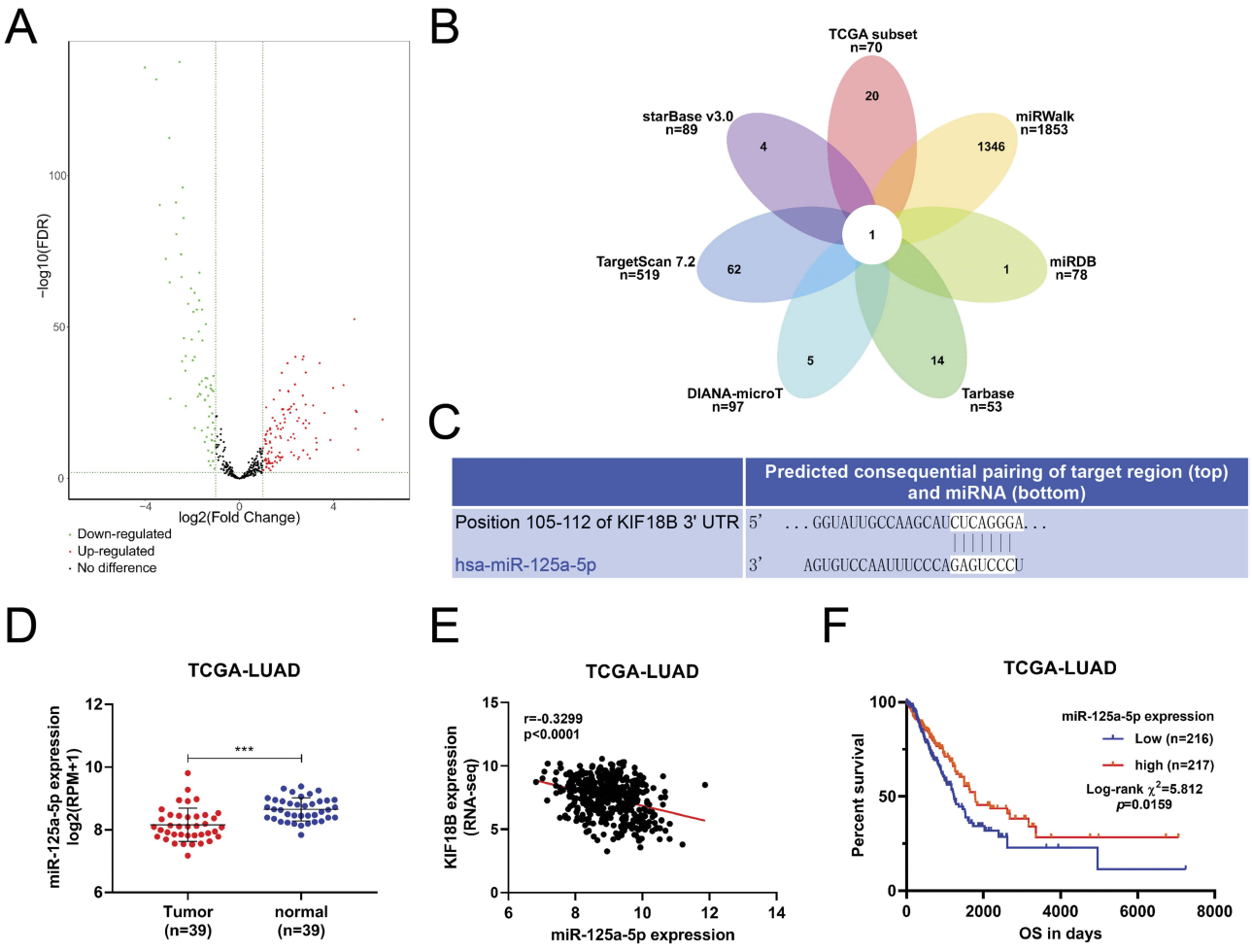

Figure 7 KIF18B was predictively targeted by hsa-miR-125a-5p in LUAD. (**A**) A volcano plot showing the differentially expressed miRNAs in TCGA-LUAD. (**B**) Venn diagram showing potential candidate regulatory miRNAs for KIF18B screened from public databases and downregulated miRNA subsets from TCGA-LUAD. (**C**) The putative binding sites in the KIF18B 3′ UTR for miR-125a-5p. (**D**) Scatter plot showing the expression of miR-125a-5p in tumor tissues and paired normal lung tissues from TCGA-LUAD. (**E**) Regression analysis of the correlation between miR-125a-5p expression and KIF18B mRNA expression. (**F**) Kaplan–Meier curves of OS in LUAD patients with high/low miR-125a-5p expression. ***$P<0.001$.

Abbreviations: KIF18B, Kinesin family member 18B; LUAD, lung adenocarcinoma; TCGA, the Cancer Genome Atlas; 3′UTR, 3′-untranslated regions; OS, overall survival.

of downregulated miRNAs, we identified hsa-miR-125a-5p to be the only overlapping miRNA (Figure 7B and C). In the paired tissues of 39 patients with LUAD, miR-125a-5p expression was lower in tumor tissue compared with normal lung tissue (Figure 7D). Linear regression analysis confirmed a significant negative correlation between miR-125a-5p expression and KIF18B mRNA expression (Figure 7E). Additionally, a Kaplan–Meier analysis suggested that low miR-125a-5p expression was significantly associated with poor OS in LUAD patients (Figure 7F).

Gene Set Enrichment Analysis Of Genes Co-Expressed With KIF18B In LUAD

To explore the potential function of KIF18B in LUAD, we analyzed RNA-seq data from 515 patients from the TCGA database via LinkedOmics. The LinkFinder module of LinkedOmics was used to analyze genes co-expressed with KIF18B in the TCGA-LUAD cohort. A total of 5590 genes (red dots) were positively correlated with KIF18B, whereas 5535 genes (green dots) were negatively correlated with KIF18B, using a cut-off of FDR <0.01 (Figure 8A). A heatmap showed the top 50 significant genes that were positively or negatively associated with KIF18B (Figure 8B and C). As shown in Figure 9A, very strong positive correlations were observed between KIF18B expression and ESPL1 expression (R=0.86), SPAG5 expression (R=0.8) and GTSE1 expression (R=0.86). Consistent with KIF18B, these three genes were upregulated in tumors compared with normal controls and were significantly correlated with poor OS in LUAD patients (Figure 9B and C).

We performed GSEA using the LinkInterpreter module of LinkedOmics. The top five significant gene ontology terms and pathway enrichment results are shown in Figure 10. The results suggest that genes positively co-expressed with KIF18B were mainly located in condensed chromosomes, chromosomal regions, spindles, midbody and microtubules, where they participated generally in chromosome segregation, DNA replication, mitotic cell cycle phase transition, spindle organization and cell cycle checkpoints. Molecular function ontology revealed that the genes were mainly enriched in GO terms such as catalytic activity (acting on DNA), helicase activity, tubulin binding, histone binding and single-stranded DNA binding (Figure 10A). Furthermore, the Kyoto Encyclopedia of Genes and Genomes (KEGG) pathway analysis showed that the significant enrichment pathways were cell cycle, homologous recombination, DNA replication, oocyte meiosis and progesterone-mediated oocyte maturation (Figures 10B and 11).

Discussion

Microtubules play an essential role in chromosome segregation, cytokinesis, vesicle trafficking and maintenance of cell polarity throughout the cell cycle.[21] As a member of the kinesin-8 family, KIF18B is a plus end-directed motor and has a second microtubule binding site in the tail.[22] Loss of KIF18B not only results in defects in spindle microtubule organization and an increase in the number and density of astral microtubules, but also disturbs chromosome alignment and perturbs microtubule dynamics in an MCAK-independent manner.[23] KIF18B is an important modulator of microtubule dynamics, but is not restricted to mitosis. Recently, specific kinesin proteins have been demonstrated as crucial in regulating mitotic events and are promising targets for cancer therapy. Although previous studies have revealed that KIF18B is upregulated

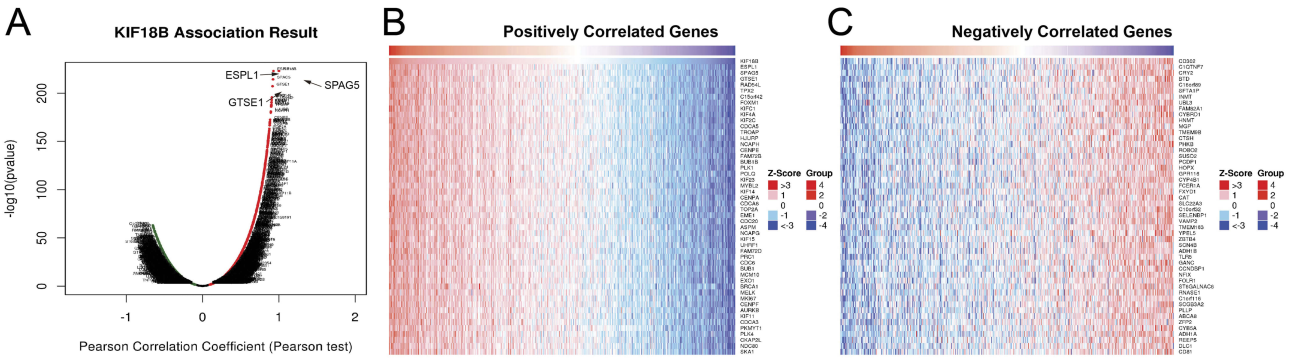

Figure 8 Differentially expressed genes correlated with KIF18B in LUAD. (**A**) A volcano plot showing differentially expressed genes significantly associated with KIF18B (FDR <0.01; *P*<0.05). (**B, C**) Heatmaps showing the top 50 significant genes positively and negatively correlated with KIF18B in LUAD.
Abbreviations: KIF18B, Kinesin family member 18B; LUAD, lung adenocarcinoma; FDR, false discovery rate.

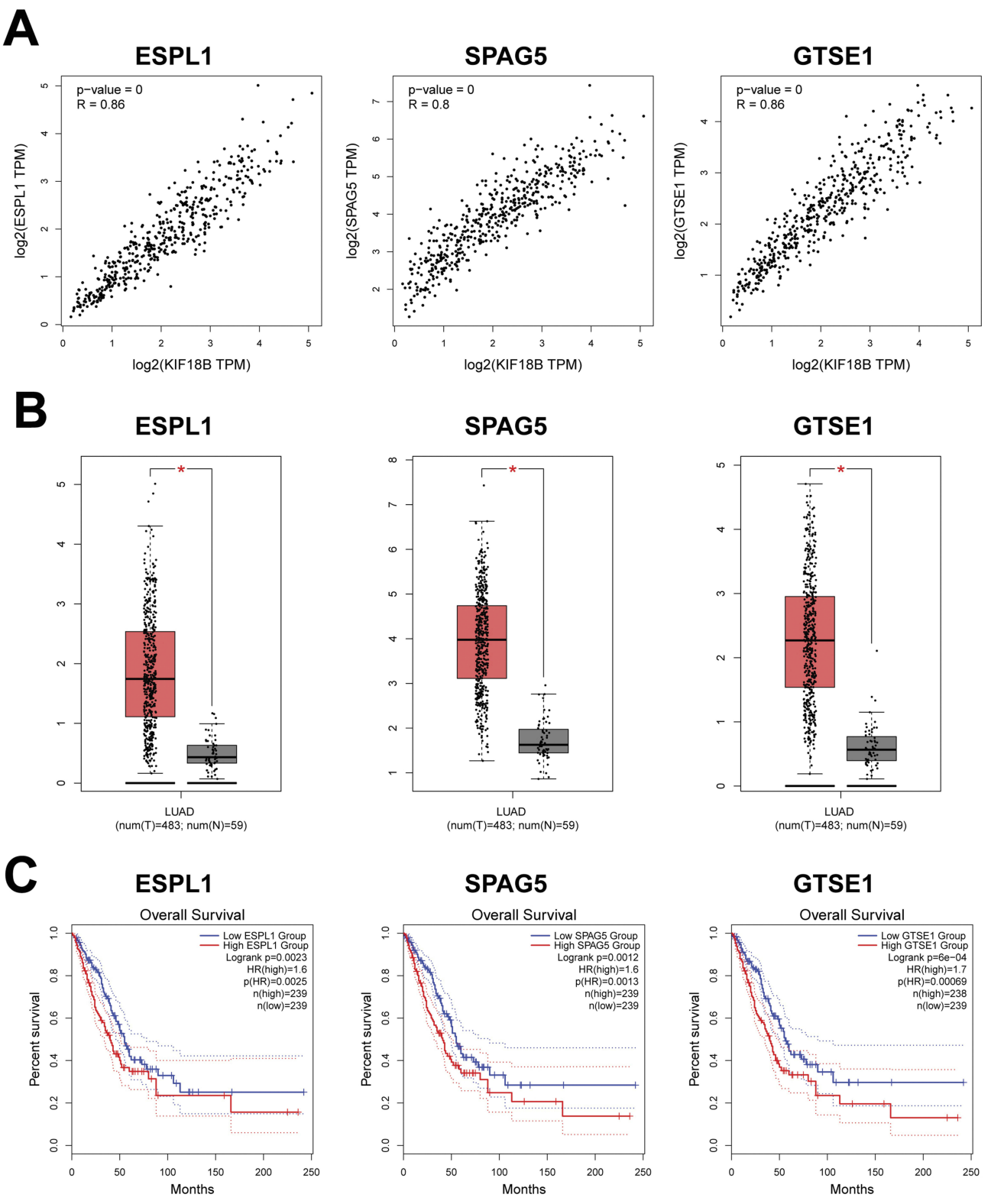

Figure 9 The top three significant genes positively co-expressed with KIF18B in LUAD. (**A**) Pearson correlation of KIF18B expression with ESPL1, SPAG5 and GTSE1 expression. (**B**) The mRNA expression profiles of ESPL1, SPAG5 and GTSE1 in LUAD tissues compared with normal lung tissues. (**C**) Survival analyses of ESPL1, SPAG5 and GTSE1 in LUAD. *P<0.05.

Abbreviations: KIF18B, Kinesin family member 18B; LUAD, lung adenocarcinoma; ESPL1, extra spindle pole bodies like 1; SPAG5, sperm associated antigen 5; GTSE1, G2 and S-phase expressed 1.

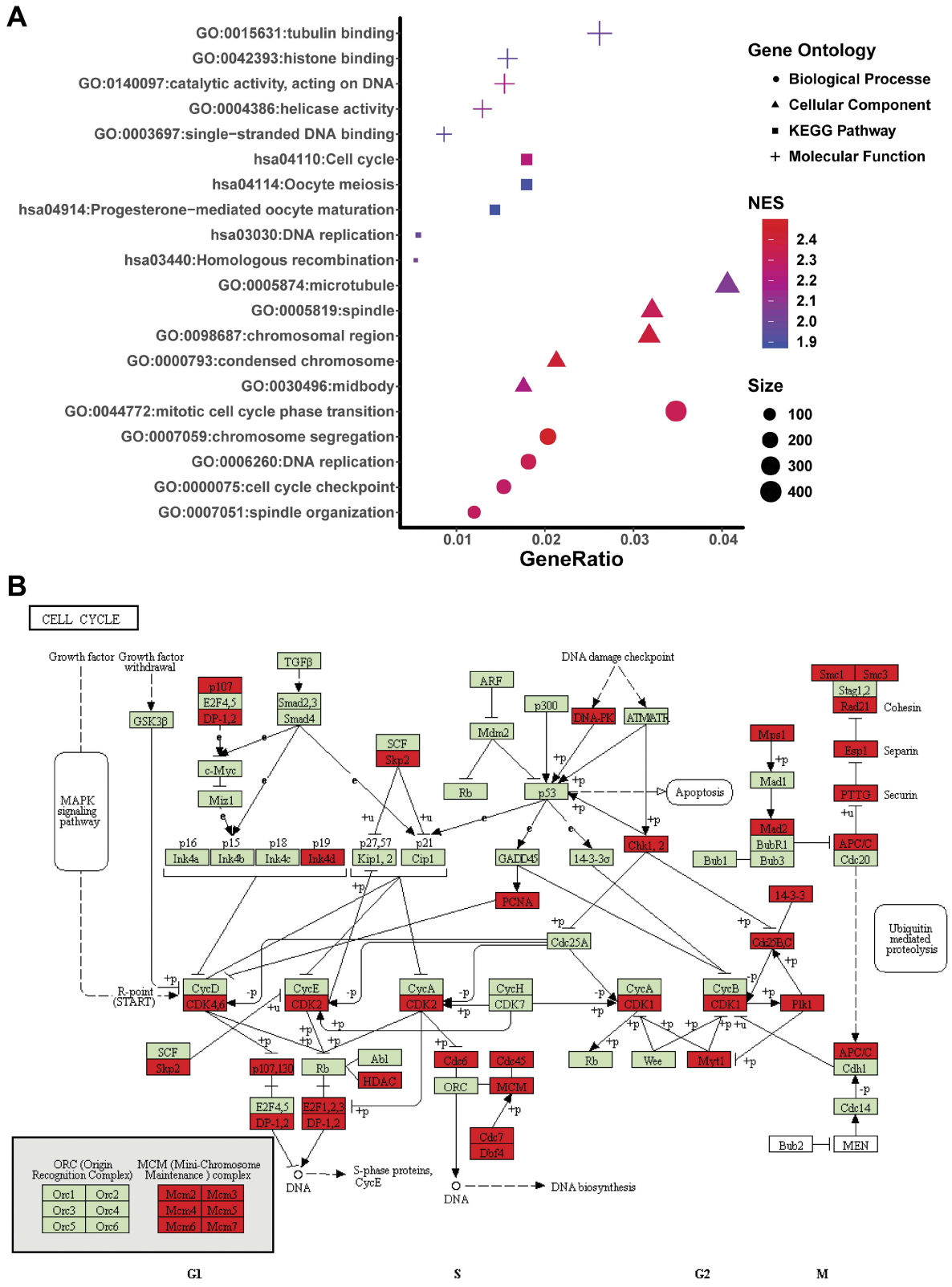

Figure 10 GO and KEGG pathway enrichment analysis of genes co-expressed with KIF18B in LUAD. (**A**) Bubble diagrams showing the top five gene ontology and KEGG pathway enrichment results of the KIF18B co-expressed genes in LUAD by GSEA. (**B**) KEGG pathway annotations of the cell cycle pathway. Red marked nodes are the associated leading-edge genes.

Abbreviations: GO, Gene Ontology; KEGG, Kyoto Encyclopedia of Genes and Genomes; KIF18B, Kinesin family member 18B; LUAD, lung adenocarcinoma; GSEA, gene set enrichment analysis.

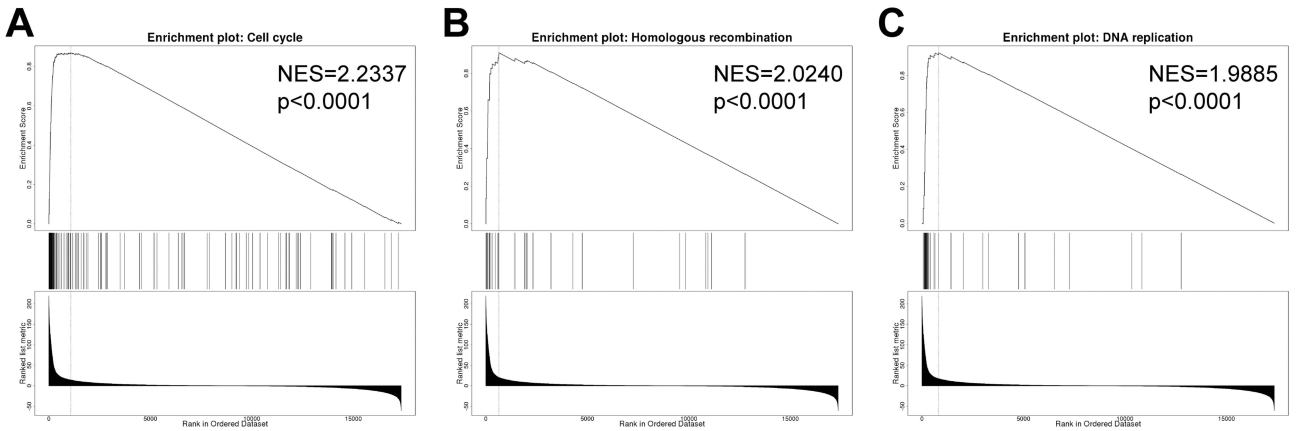

Figure 11 GSEA based on TCGA-LUAD dataset. KIF18B upregulation was associated with "Cell cycle" (**A**), "Homologous recombination" (**B**) and "DNA replication" (**C**).
Abbreviations: GSEA, gene set enrichment analysis; TCGA, the Cancer Genome Atlas; LUAD, lung adenocarcinoma; KIF18B, Kinesin family member 18B.

in several human cancers.[7,24] The expression profiles, clinical significance and potential molecular mechanism of KIF18B in LUAD have not yet been reported.

In the current study, we firstly revealed that KIF18B expression was upregulated both at mRNA and protein levels in LUAD tissues compared with normal lung tissues. These results were consistent with those obtained through data mining in TCGA and GEO databases. KIF18B was remarkably increased in most human solid tumors, including LUAD, suggesting that KIF18B might act as an oncogene in LUAD. Based on ROC curves, KIF18B mRNA and protein expression demonstrated reliable diagnostic value, which indicated that KIF18B might be a promising biomarker for LUAD diagnosis. Tooker et al[25] found that reduced concentrations of KIF18A protein in the serum of asbestosis patients who developed cancer could be used as a blood biomarker to identify asbestosis patients at risk of developing lung cancer. However, it is unclear whether aberrant levels of serum KIF18B exist in LUAD patients. Wu et al[7] found that KIF18B was upregulated in cervical cancer and was correlated with a large tumor size and an advanced clinical stage. We further explored the clinical significance of KIF18B mRNA expression in LUAD. KIF18B mRNA expression was higher in males and in smokers. Moreover, high KIF18B expression was significantly associated with positive nodal invasion, advanced TNM stage and death status. KIF18B might be involved in the carcinogenesis and progression of LUAD. Notably, overexpression of KIF18B promoted cell proliferation, migration and invasion in cervical cancer, and silencing it could reverse these effects.[7] Whether KIF18B has the same biological function in lung cancer requires further experimental confirmation. In addition, we found that KIF18B overexpression was associated with poorer OS and RFS in LUAD. Based on univariate and multivariate Cox analyses, high KIF18B expression was an independent predictor of unfavorable OS and RFS. The prognostic value of KIF18B in predicting OS and RFS in LUAD was also validated by ROC curves. KIF18B has also been confirmed to be associated with significantly worse OS in hepatocellular carcinoma.[8,26] Our results indicated that KIF18B expression might serve as a specific and promising prognostic indicator in patients with LUAD.

To the best of our knowledge, the underlying molecular mechanisms of KIF18B dysregulation in tumors have not yet been fully elucidated. Considering the potential diagnostic and prognostic value of KIF18B in LUAD, it is meaningful to explore the underlying mechanism of its dysregulation in LUAD. Genetic and epigenetic alterations, such as CNVs and DNA methylation, are quite common in cancers and may have a profound influence on tumor phenotypes and patient survival.[27] CNVs can regulate the expression of a specific gene through dose effects,[28] while DNA methylation frequently occurs at CpG islands and is linked to the activation of oncogenes and the inhibition of tumor suppressor genes.[29–31] In the present study, consistent with KIF18A,[5] DNA amplification was the major type of KIF18B alteration observed in LUAD and was positively associated with the upregulation of KIF18B. This relationship between CNVs and KIF18B mRNA expression was also confirmed in LUAD cell lines. Therefore, we speculated that aberrant KIF18B expression and dysregulation in LUAD might result from alterations

in chromosomal structure. Moreover, the methylation level of some CpG sites was lower in LUAD tissues and was negatively correlated with KIF18B expression. These results suggest that KIF18B expression might be modulated by DNA methylation in LUAD.

MicroRNAs (miRNAs) are single-stranded noncoding RNAs and have long been known to play a key role in gene expression regulation.[32,33] Some miRNAs, which are downregulated in cancers, generally bind to the 3′-untranslated regions (3′UTR) of their target mRNAs,[33] and silence genes by inducing mRNA degradation or preventing translation of mRNA.[34,35] Here, we identified miR-125a-5p as potentially regulating KIF18B expression using public prediction databases and experimentally validated databases. As the only candidate miRNA, miR-125a-5p was significantly downregulated in LUAD tissues compared with paired normal lung tissues and was negatively correlated with KIF18B mRNA expression. Previous studies have confirmed that miR-125a-5p is downregulated in some cancers including lung cancer and that it acts as a tumor suppressor.[36] Overexpressing miR-125a-5p can self-activate silenced miR-125a-5p in lung cancer cells, which suppresses cell proliferation, migration and invasion, and inhibits cancer progression.[37,38] Additionally, our results revealed that low miR-125a-5p expression was significantly correlated with shorter OS in LUAD, which is consistent with previous studies.[39] Given that miR-125a-5p could bind to the putative binding site of the KIF18B 3′UTR, our results suggest that miR-125a-5p might be the upstream regulator of KIF18B, providing a new mechanism for the dysregulation of KIF18B in LUAD. Of course, validating these findings will require further experimentation, such as using a dual-luciferase reporter assay to confirm this interaction.

In addition, we explored the underlying biological function and molecular mechanisms that underpin the potential clinical value of KIF18B in LUAD. The genes co-expressed with KIF18B in LUAD were identified on the web-based platform of the LinkedOmics database. The most significant positively correlated genes were ESPL1, SPAG5 and GTSE1, which were overexpressed in tumor tissues and linked to poor OS in patients with LUAD. Indeed, ESPL1,[40,41] SPAG5,[42,43] and GTSE1[44] have been reported as oncogenes in various human cancers, including lung cancer.

GO and KEGG pathway enrichment analyses of genes positively co-expressed with KIF18B in LUAD were analyzed using GSEA. Gene functional enrichment analysis suggested that these genes were dominantly enriched in the chromosome, spindle and microtubule, and primarily participated in cell cycle-related activities and regulation, such as mitotic cell cycle phase transition, chromosome segregation and cell cycle checkpoint activities. Similarly, "cell cycle" was the most significant signaling pathway for KIF18B co-expressed genes enriched in LUAD. The cell cycle plays a significant role in tumorigenesis.[45] Dysregulation of cell cycle can result in cancer cell proliferation and tumor growth.[46] A variety of molecules, including kinesins, have been reported to be involved in cell cycle dysregulation.[47–49] Silencing of KIF18A, a homolog of KIF18B, induced LUAD cell apoptosis and arrested the cell cycle in the G2/M phase.[5] Interestingly, KIF18B significantly promoted cell proliferation and tumorigenesis in cervical cancer.[7] Knockdown of KIF18B induced cell cycle G1 – phase arrest, inhibited cell cycle progression by decreasing CyclinD1 expression and suppressing expression of Wnt/β-catenin pathway-related proteins.[7] KIF18B expression is modulated in a cell cycle-dependent manner and may play an important role in cell division. These findings are consistent with the physiological function of the KIF18B gene. KIF18B might function as a novel oncogene via the cell cycle regulation pathway in LUAD.

There were some limitations to the current study. Firstly, our results were validated using the GEO datasets, which contain relatively small sample sizes, with relatively few stage IV patients. Secondly, transcriptomics analysis does not reflect protein activity or expression levels, which are crucial for genes to produce a biological effect. Thirdly, the molecular mechanism results are based on bioinformatics analysis, meaning that there is a lack of in vitro and in vivo experiments. However, our findings have provided new insights into the development and treatment of lung cancer. In future work, we will perform in-depth studies to validate our current findings.

Conclusion

In summary, KIF18B was upregulated in LUAD tissues compared with normal lung tissues. Increased expression of KIF18B was associated with unfavorable clinicopathological features and independently predicted poor prognosis in patients with LUAD. DNA amplification, hypomethylation and miRNA-125a-5p downregulation might contribute to KIF18B dysregulation in LUAD. KIF18B might act as an oncogene in LUAD by affecting the cell cycle pathway. KIF18B might be a potential therapeutic target for lung cancer.

Acknowledgments

This work was funded by the National Natural Science Foundation of China (81560383, 81360020), Guangxi Natural Science Foundation (2018GXNSFBA281058), Guangxi Key Research and Development Program (AB16380226) and the self-financing research projects of Guangxi Zhuang Autonomous Region (Z20170353). We thank the Pathology Department of The People's Hospital of Guangxi Zhuang Autonomous Region.

Disclosure

The authors report no conflicts of interest in this work.

References

1. Siegel RL, Miller KD, Jemal A. Cancer statistics, 2019. *CA Cancer J Clin*. 2019;69(1):7–34. doi:10.3322/caac.21551
2. Miller KD, Siegel RL, Lin CC, et al. Cancer treatment and survivorship statistics, 2016. *CA Cancer J Clin*. 2016;66(4):271–289. doi:10.3322/caac.21349
3. Miki H, Setou M, Kaneshiro K, Hirokawa N. All kinesin superfamily protein, KIF, genes in mouse and human. *Proc Natl Acad Sci*. 2001;98(13):7004–7011. doi:10.1073/pnas.111145398
4. Yu Y, Feng Y. The role of kinesin family proteins in tumorigenesis and progression. *Cancer Am Cancer Soc*. 2010;116(22):5150–5160.
5. Zhong Y, Jiang L, Lin H, et al. Overexpression of KIF18A promotes cell proliferation, inhibits apoptosis, and independently predicts unfavorable prognosis in lung adenocarcinoma. *IUBMB Life*. 2019;71(7):942–955. doi:10.1002/iub.2030
6. Stout JR, Yount AL, Powers JA, Leblanc C, Ems-Mcclung SC, Walczak CE. Kif18B interacts with EB1 and controls astral microtubule length during mitosis. *Mol Biol Cell*. 2011;22(17):3070–3080. doi:10.1091/mbc.E11-04-0363
7. Wu Y, Wang A, Zhu B, et al. KIF18B promotes tumor progression through activating the Wnt/beta-catenin pathway in cervical cancer. *Onco Targets Ther*. 2018;11:1707–1720. doi:10.2147/OTT.S157440
8. Xiang X, Yang L, Zhang X, et al. Seven-senescence-associated gene signature predicts overall survival for Asian patients with hepatocellular carcinoma. *World J Gastroenterol*. 2019;25(14):1715–1728. doi:10.3748/wjg.v25.i14.1715
9. Chandrashekar DS, Bashel B, Balasubramanya S, et al. UALCAN: a portal for facilitating tumor subgroup gene expression and survival analyses. *Neoplasia*. 2017;19(8):649–658. doi:10.1016/j.neo.2017.05.002
10. Barrett T, Troup DB, Wilhite SE, et al. NCBI GEO: archive for high-throughput functional genomic data. *Nucleic Acids Res*. 2009;37(Database issue):D885–D890. doi:10.1093/nar/gkn764
11. Ghandi M, Huang FW, Jane-Valbuena J, et al. Next-generation characterization of the cancer cell line encyclopedia. *Nature*. 2019;569(7757):503–508. doi:10.1038/s41586-019-1186-3
12. Barretina J, Caponigro G, Stransky N, et al. The cancer cell line encyclopedia enables predictive modelling of anticancer drug sensitivity. *Nature*. 2012;483(7391):603–607. doi:10.1038/nature11003
13. Sticht C, De La Torre C, Parveen A, Gretz N, Campbell M. miRWalk: an online resource for prediction of microRNA binding sites. *PLoS One*. 2018;13(10):e206239. doi:10.1371/journal.pone.0206239
14. Liu W, Wang X. Prediction of functional microRNA targets by integrative modeling of microRNA binding and target expression data. *Genome Biol*. 2019;20(1):18. doi:10.1186/s13059-019-1629-z
15. Karagkouni D, Paraskevopoulou MD, Chatzopoulos S, et al. DIANA-TarBase v8: a decade-long collection of experimentally supported miRNA-gene interactions. *Nucleic Acids Res*. 2018;46(D1):D239–D245. doi:10.1093/nar/gkx1141
16. Paraskevopoulou MD, Georgakilas G, Kostoulas N, et al. DIANA-microT web server v5.0: service integration into miRNA functional analysis workflows. *Nucleic Acids Res*. 2013;41:W169-W173.
17. Agarwal V, Bell GW, Nam JW, Bartel DP. Predicting effective microRNA target sites in mammalian mRNAs. *Elife*. 2015;4:e05005. doi:10.7554/eLife.06416
18. Li JH, Liu S, Zhou H, Qu LH, Yang JH. starBase v2.0: decoding miRNA-ceRNA, miRNA-ncRNA and protein-RNA interaction networks from large-scale CLIP-Seq data. *Nucleic Acids Res*. 2014;42(Database issue):D92–D97. doi:10.1093/nar/gkt1248
19. Vasaikar SV, Straub P, Wang J, Zhang B. LinkedOmics: analyzing multi-omics data within and across 32 cancer types. *Nucleic Acids Res*. 2018;46(D1):D956–D963. doi:10.1093/nar/gkx1090
20. Tang Z, Kang B, Li C, Chen T, Zhang Z. GEPIA2: an enhanced web server for large-scale expression profiling and interactive analysis. *Nucleic Acids Res*. 2019;47(W1):W556–W560. doi:10.1093/nar/gkz430
21. Messin LJ, Millar JBA. Role and regulation of kinesin-8 motors through the cell cycle. *Syst Synth Biol*. 2014;8(3):205–213. doi:10.1007/s11693-014-9140-z
22. Shin Y, Du Y, Collier SE, Ohi MD, Lang MJ, Ohi R. Biased brownian motion as a mechanism to facilitate nanometer-scale exploration of the microtubule plus end by a kinesin-8. *Proc Natl Acad Sci U S A*. 2015;112(29):E3826–E3835. doi:10.1073/pnas.1500272112
23. Walczak CE, Zong H, Jain S, Stout JR. Spatial regulation of astral microtubule dynamics by Kif18B in PtK cells. *Mol Biol Cell*. 2016;27(20):3021–3030. doi:10.1091/mbc.E16-04-0254
24. Itzel T, Scholz P, Maass T, et al. Translating bioinformatics in oncology: guilt-by-profiling analysis and identification of KIF18B and CDCA3 as novel driver genes in carcinogenesis. *Bioinformatics*. 2015;31(2):216–224.
25. Tooker BC, Newman LS, Bowler RP, et al. Proteomic detection of cancer in asbestosis patients using SELDI-TOF discovered serum protein biomarkers. *Biomarkers*. 2010;16(2):181–191. doi:10.3109/1354750X.2010.543289
26. Schiewek J, Schumacher U, Lange T, et al. Clinical relevance of cytoskeleton associated proteins for ovarian cancer. *J Cancer Res Clin*. 2018;144(11):2195–2205. doi:10.1007/s00432-018-2710-9
27. Gao Y, Teschendorff AE. Epigenetic and genetic deregulation in cancer target distinct signaling pathway domains. *Nucleic Acids Res*. 2017;45(2):583–596. doi:10.1093/nar/gkw1100
28. Gamazon ER, Stranger BE. The impact of human copy number variation on gene expression. *Brief Funct Genomics*. 2015;14(5):352–357. doi:10.1093/bfgp/elv017
29. Perri F, Longo F, Giuliano M, et al. Epigenetic control of gene expression: potential implications for cancer treatment. *Crit Rev Oncol Hematol*. 2017;111:166–172. doi:10.1016/j.critrevonc.2017.01.020
30. Moore LD, Le T, Fan G. DNA methylation and its basic function. *Neuropsychopharmacol*. 2013;38(1):23–38. doi:10.1038/npp.2012.112
31. Nakamura J, Tanaka T, Kitajima Y, Noshiro H, Miyazaki K. Methylation-mediated gene silencing as biomarkers of gastric cancer: a review. *World J Gastroenterol*. 2014;20(34):11991–12006. doi:10.3748/wjg.v20.i34.11991
32. Lewis BP, Burge CB, Bartel DP. Conserved seed pairing, often flanked by adenosines, indicates that thousands of human genes are microRNA targets. *Cell*. 2005;120(1):15–20. doi:10.1016/j.cell.2004.12.035
33. Chen K, Rajewsky N. The evolution of gene regulation by transcription factors and microRNAs. *Nat Rev Genet*. 2007;8(2):93–103. doi:10.1038/nrg1990
34. Djuranovic S, Nahvi A, Green R. miRNA-mediated gene silencing by translational repression followed by mRNA deadenylation and decay. *Science*. 2012;336(6078):237–240. doi:10.1126/science.1215691
35. Cannell IG, Kong YW, Bushell M. How do microRNAs regulate gene expression? *Biochem Soc Trans*. 2008;36(Pt 6):1224–1231. doi:10.1042/BST0361224

36. Zheng H, Wu J, Shi J, et al. miR-125a-5p upregulation suppresses the proliferation and induces the cell apoptosis of lung adenocarcinoma by targeting NEDD9. *Oncol Rep*. 2017;38(3):1790–1796. doi:10.3892/or.2017.5812
37. Jiang L, Huang Q, Zhang S, et al. Hsa-miR-125a-3p and hsa-miR-125a-5p are downregulated in non-small cell lung cancer and have inverse effects on invasion and migration of lung cancer cells. *BMC Cancer*. 2010;10:318. doi:10.1186/1471-2407-10-663
38. Liu H, Ma Y, Liu C, Li P, Yu T. Reduced miR-125a-5p level in non-small-cell lung cancer is associated with tumour progression. *Open Biol*. 2018;8(10):180118. doi:10.1098/rsob.180118
39. Zhu WY, Luo B, An JY, et al. Differential expression of miR-125a-5p and let-7e predicts the progression and prognosis of non-small cell lung cancer. *Cancer Invest*. 2014;32(8):394–401. doi:10.3109/07357907.2014.922569
40. Finetti P, Guille A, Adelaide J, Birnbaum D, Chaffanet M, Bertucci F. ESPL1 is a candidate oncogene of luminal B breast cancers. *Breast Cancer Res Treat*. 2014;147(1):51–59. doi:10.1007/s10549-014-3070-z
41. He X, Zhang C, Shi C, Lu Q. Meta-analysis of mRNA expression profiles to identify differentially expressed genes in lung adenocarcinoma tissue from smokers and non-smokers. *Oncol Rep*. 2018;39(3):929–938. doi:10.3892/or.2018.6197
42. Yang YF, Zhang MF, Tian QH, et al. SPAG5 interacts with CEP55 and exerts oncogenic activities via PI3K/AKT pathway in hepatocellular carcinoma. *Mol Cancer*. 2018;17(1):117. doi:10.1186/s12943-018-0872-3
43. Wang T, Li K, Song H, et al. p53 suppression is essential for oncogenic SPAG5 upregulation in lung adenocarcinoma. *Biochem Biophys Res Commun*. 2019;513(2):319–325. doi:10.1016/j.bbrc.2019.03.198
44. Wu X, Wang H, Lian Y, et al. GTSE1 promotes cell migration and invasion by regulating EMT in hepatocellular carcinoma and is associated with poor prognosis. *Sci Rep*. 2017;7(1):5129. doi:10.1038/s41598-017-05311-2
45. Ingham M, Schwartz GK. Cell-cycle therapeutics come of age. *J Clin Oncol*. 2017;35(25):2949–2959. doi:10.1200/JCO.2016.69.0032
46. Malumbres M, Barbacid M. Cell cycle, CDKs and cancer: a changing paradigm. *Nat Rev Cancer*. 2009;9(3):153–166. doi:10.1038/nrc2602
47. Wang ZZ, Yang J, Jiang BH, et al. KIF14 promotes cell proliferation via activation of Akt and is directly targeted by miR-200c in colorectal cancer. *Int J Oncol*. 2018;53(5):1939–1952. doi:10.3892/ijo.2018.4546
48. Hou P, Jiang T, Chen F, et al. KIF4A facilitates cell proliferation via induction of p21-mediated cell cycle progression and promotes metastasis in colorectal cancer. *Cell Death Dis*. 2018;9(5):477. doi:10.1038/s41419-018-1111-y
49. Xie T, Li X, Ye F, et al. High KIF2A expression promotes proliferation, migration and predicts poor prognosis in lung adenocarcinoma. *Biochem Bioph Res Co*. 2018;497(1):65–72. doi:10.1016/j.bbrc.2018.02.020